

PAPER

## Sub-200 ps spin transfer torque switching in in-plane magnetic tunnel junctions with interface perpendicular anisotropy

To cite this article: Hui Zhao *et al* 2012 *J. Phys. D: Appl. Phys.* **45** 025001

View the [article online](#) for updates and enhancements.

### Related content

- [Low-power non-volatile spintronic memory: STT-RAM and beyond](#)  
K L Wang, J G Alzate and P Khalili Amiri
- [Low current density induced spin-transfer torque switching in CoFeB–MgO magnetic tunnel junctions with perpendicular anisotropy](#)  
H Meng, R Sbiaa, S Y H Lua *et al.*
- [Direct characterization of spin-transfer switching of nano-scale magnetic tunnel junctions using a conductive atomic force microscope](#)  
Jia-Mou Lee, Dong-Chin Yang, Ching-Ming Lee *et al.*

### Recent citations

- [Time-resolved imaging of pulse-induced magnetization reversal with a microwave assist field](#)  
Siddharth Rao *et al*
- [Tunnel Junction with Perpendicular Magnetic Anisotropy: Status and Challenges](#)  
Mengxing Wang *et al*
- [Jian-Ping Wang \*et al\*](#)

# Sub-200 ps spin transfer torque switching in in-plane magnetic tunnel junctions with interface perpendicular anisotropy

Hui Zhao<sup>1</sup>, Brian Glass<sup>2</sup>, Pedram Khalili Amiri<sup>3</sup>, Andrew Lyle<sup>1</sup>,  
Yisong Zhang<sup>1</sup>, Yu-Jin Chen<sup>4</sup>, Graham Rowlands<sup>4</sup>, Pramey Upadhyaya<sup>3</sup>,  
Zhongming Zeng<sup>5</sup>, J A Katine<sup>6</sup>, Juergen Langer<sup>7</sup>, Kosmas Galatsis<sup>3</sup>,  
Hongwen Jiang<sup>5</sup>, Kang L Wang<sup>3</sup>, Ilya N Krivorotov<sup>4</sup> and  
Jian-Ping Wang<sup>1,2</sup>

<sup>1</sup> Electrical and Computer Engineering, University of Minnesota, Minneapolis, MN 55455, USA

<sup>2</sup> Physics and Astronomy, University of Minnesota, Minneapolis, MN 55455, USA

<sup>3</sup> Electrical Engineering, University of California, Los Angeles, CA 90095, USA

<sup>4</sup> Physics and Astronomy, University of California, Irvine, CA 92697, USA

<sup>5</sup> Physics and Astronomy, University of California, Los Angeles, CA 90095, USA

<sup>6</sup> Hitachi Global Storage Technologies, 3403 Yerba Buena Road, San Jose, CA 95135, USA

<sup>7</sup> Singulus Technologies, 63796 Kahl am Main, Germany

E-mail: [jpwang@umn.edu](mailto:jpwang@umn.edu)

Received 4 October 2011, in final form 17 November 2011

Published 20 December 2011

Online at [stacks.iop.org/JPhysD/45/025001](http://stacks.iop.org/JPhysD/45/025001)

## Abstract

Ultrafast spin transfer torque (STT) switching in an in-plane MgO magnetic tunnel junction with  $50\text{ nm} \times 150\text{ nm}$  elliptical shape was demonstrated in this paper. Switching speeds as short as 165 ps and 190 ps at 50% and 98% switching probabilities, respectively, were observed without external field assistance in a thermally stable junction with a 101% tunnelling magnetoresistance ratio. The minimum writing energy of P-AP switching for 50% and 98% switching probability are 0.16 pJ and 0.21 pJ, respectively. The observed ultrafast switching is believed to occur because of partially cancelled out-of-plane demagnetizing field in the free layer from interface perpendicular anisotropy between the MgO layer and the  $\text{Co}_{20}\text{Fe}_{60}\text{B}_{20}$  layer. High  $J/J_{c0}$  ratio and magnetization nucleation at the edge of free layer, which result from the reduced perpendicular demagnetizing field, are possibly two major factors that contribute to the ultrafast STT switching.

(Some figures may appear in colour only in the online journal)

Ultrafast spin transfer torque (STT) switching in the sub-ns regime is one of the key issues for spin transfer torque random access memory (STT-RAM) development. One of the crucial limitations for ultrafast switching is the incubation delay induced by pre-switching oscillation [1]. Several approaches have been proposed to minimize pre-switching oscillations in order to improve the switching speed in spin valves (SVs), such as developing all perpendicular structures [2], applying hard axis field to set the free layer equilibrium away from the easy axis [3], and adding an extra perpendicular polarizer [4–6]. As of now, limited work has been done on sub-nanosecond STT switching in magnetic tunnel junctions

(MTJs). Minimum switching times of 400–580 ps at 50% switching probability has been reported in conventional in-plane MTJs [7, 8]. By adding perpendicular polarizer, Liu *et al* showed 100% switching at 500 ps with external field assistance in their MTJ+SV device [9]. Rowlands *et al* achieved 50% switching probability at 120 ps under zero bias field in the full orthogonal MTJ [10].

In this paper, we report ultrafast switching (165 ps–10 ns) in CoFeB–MgO MTJs with good tunnelling magnetoresistance (TMR) ratio around 100% and large coercivity (100 Oe) under zero bias field. With a basic conventional stack structure, the sample exhibits ultrafast switching in the sub-200 ps

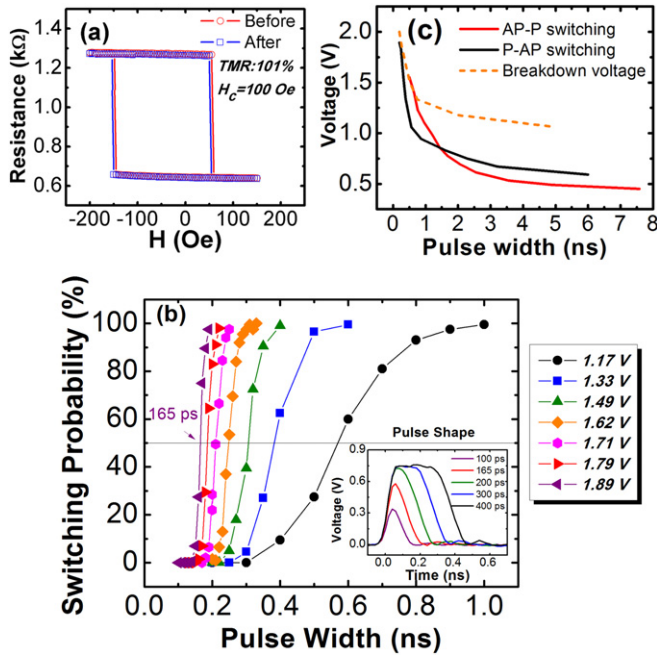


**Figure 1.** (a) MTJ resistance versus magnetic field loop at room temperature. The red curve is tested before switching probability measurement and the blue curve is obtained after switching probability measurement. (b) Switching probability dependence on pulse width with various pulse amplitudes on P-AP side. Each curve corresponds to the same setting voltage on pulse generator. The inset figure shows the change in pulse shape from 100 to 400 ps with the same setting amplitude. Because of the pulse peak attenuation, the labelled voltage in figure 1(b) is the peak voltage at the pulse duration corresponding to 50% switching probability<sup>8</sup>. For example, the first curve (purple, triangle-to-left) has the nominal pulse amplitude at 2.4 V for long pulses. The labelled value is 1.89 V, which means the peak value at 165 ps pulse width with 50% switching probability. (c) Pulse voltage as a function of pulse width at 50% switching probability for AP-P and P-AP switching. And the dashed line is the breakdown voltage at different pulse widths.

regime while maintaining all the requirements for STT-RAM application.

The MTJ samples' stacking structure is as follows: (bottom electrode)/PtMn (15 nm)/Co<sub>70</sub>Fe<sub>30</sub> (2.3 nm)/Ru (0.85 nm)/Co<sub>40</sub>Fe<sub>40</sub>B<sub>20</sub> (2.4 nm)/MgO (0.83 nm)/Co<sub>20</sub>Fe<sub>60</sub>B<sub>20</sub> (1.7–2.0 nm)/(top electrode). Here we used Fe-rich free layer from 1.7 to 2.0 nm, which has a strong perpendicular interface anisotropy [11, 12], but still retains the easy axis in plane. The sample was post-annealed at 300 °C under 1 T magnetic field for 2 h. MTJ devices in this paper were patterned into 50 nm × 150 nm elliptical nanopillars.

The samples were characterized at room temperature for resistance versus applied field (*R–H*) loop and switching probability. The switching probability measurement was performed by a sequence similar to our previous work [8] under zero bias field. Each probability value was calculated by 200 switching trials with the free layer magnetization preset by a 1 μs reset pulse. The 100 ps–10 ns switching pulse was generated by the picosecond bipolar voltage pulse generator 10070A, which has a rise and fall time of 65 ps and 85 ps, respectively.

Figure 1(a) shows the *R–H* loop of a MTJ sample with 2.0 nm free layer. The sample has the TMR ratio of 101%

and the coercivity of 100 Oe. By averaging from a group of similar devices, the thermal stability is estimated to be above 65 *k<sub>B</sub>T* according to the hard-axis magnetoresistance curve fitting method [13]. The loop is centred at –45 Oe due to the coupling with pinned layer which is compensated by an external field during all the following switching probability measurements. The nearly overlapping blue and red *R–H* loops were obtained before and after the switching probability measurement, respectively, and showed that no partial breakdown of the barrier or change of magnetic properties had occurred.

The switching probability as a function of pulse width is plotted in figure 1(b), where each curve represents the setting same pulse amplitude. The labelled voltage is the pulse peak voltage on the device at the pulse duration corresponding to 50% switching probability<sup>8</sup>. Please find more description in the figure caption of figure 1(b) and footnote 8. We observed 50% switching probability at 165 ps and 98% switching probability at 190 ps. Moreover, the switching probability curves were very steep and did not display a switching probability plateau because of the half precession period jitter as observed in some metallic SVs [1]. Furthermore, the observed sub-200 ps switching implies that incubation delay did not occur as a result of pre-switching oscillation. To calculate the writing energy, we did an integration based on the pulse shape for each pulse width by  $E_w = \int V^2(t)/R dt$ . The minimum writing energy of P-AP switching for 50% and 98% switching probabilities are 0.16 pJ and 0.21 pJ, respectively. During the measurement, the samples can generally survive 10<sup>3</sup>–10<sup>4</sup> writing circles for the sub-200 ps switching. And we also calculated the endurance in our sample according to [14], with 1.107 V, 500 ps pulse width, the failure rate is 3.25 × 10<sup>–4</sup>.

The same switching probability measurement was also done for AP-P switching. We plot the pulse amplitude versus pulse width at 50% probability in figure 1(c) together with the breakdown voltage, which was measured from 20 MTJs' breakdown point with identical barrier thickness at various pulse widths. The figure shows that the achievable minimum switching time is limited by the breakdown voltage of the device. With the same applied voltage, the current through the device in the P state is about twice the value in the AP state due to the resistance difference in each state. Therefore, for P-AP switching higher voltages can be reached, thus allowing shorter switching times, as shown in figure 1(c).

Two other MTJs of the same size but with thinner free layers (1.90 nm, 1.73 nm) were also measured for ultrafast switching probabilities in the sub-ns regime. The results were summarized in figure 2. The red line indicates the current density at which the oxide barrier breaks down at different pulse widths. Again, we see that the minimum measured switching time is limited by the breakdown voltage, especially

<sup>8</sup> For pulses below 300 ps, the pulse shape turns to triangle as shown in the inset of figure 1(b) from equipment constraints and the peak voltage starts to decrease with pulse width. Therefore, with the same setting voltage, real pulse voltage varies in the ultrafast switching end. For example, at 165 ps pulse width, the 2.4 V nominal pulse amplitude is reduced to 1.89 V. All the pulse voltage values used in this paper are the peak voltage measured by Tektronix DPO72004BO scilloscope (20 GHz bandwidth and 50 GHz sampling rate) multiplied by the reflection coefficient at the MTJ end ( $\Gamma = 2R_{MTJ}/(R_{MTJ} + Z_0)$ ).

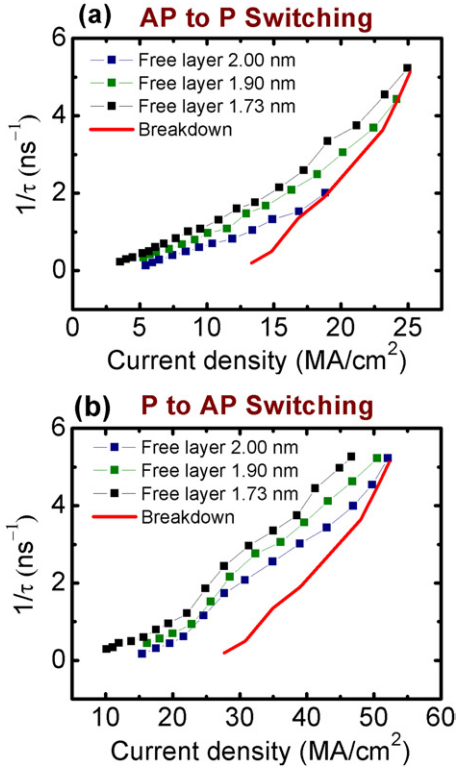


**Figure 2.** The inverse of pulse width as a function of current density for AP-P switching (a) and P-AP switching (b). The red curve indicates equivalent breakdown current density at various pulse widths.

in the AP-P switching case due to its higher resistance. For the 1.73 nm free layer sample, we found 50% switching probability at 195 ps for AP-P switching, and 190 ps for P-AP switching, corresponding to 0.12 pJ and 0.23 pJ writing energy, respectively.

According to the macrospin approximation of STT switching theory, the precessional switching time is inversely proportional to the applied current density [15].

$$\tau^{-1} \approx \frac{\hbar\eta}{2eM_s H_k t \ln(\pi/2\theta_0)} (J - J_{c0}), \quad (1)$$

where  $\eta$  is the spin polarization,  $M_s$  is the free layer magnetization,  $H_k$  is the in-plane easy axis anisotropy field,  $t$  is the free layer thickness,  $\theta_0$  is the initial angle between the free layer and pinned layer and  $J_{c0}$  is the intrinsic critical current density.

The linear relationships in figures 2(a) and (b), between  $\tau^{-1}$  and  $J$  at  $\tau^{-1} > 1 \text{ ns}^{-1}$  show that with such a short pulse duration, the switching process is mainly precessional switching. In the regime of  $\tau^{-1} < 1 \text{ ns}^{-1}$ , thermal activation starts to contribute to STT switching, leading the tails near zero to gradually become more shallow as less current density is needed for switching. Furthermore, as the free layer thickness decreases from 2.00 to 1.73 nm, the curves shift from right to left indicating a reduction in  $J_{c0}$ .

It is noteworthy to point out that in our basic in-plane MgO MTJ structure, the demonstrated switching speed of 165 ps (50%) and 190 ps (98%) is surprisingly similar to

the value in orthogonal MTJs [9, 10]. We propose here that the observed ultrafast STT switching mainly benefits from interface perpendicular anisotropy between the MgO layer and the  $\text{Co}_{20}\text{Fe}_{60}\text{B}_{20}$  layer [11]. As a result, the out-of-plane demagnetizing field in the free layer is partially cancelled. In our sample, interface perpendicular anisotropy  $K_{in}$  is calibrated by VSM measurement as  $2.4 \text{ erg cm}^{-2}$  [12]. We define  $H_d$  as the out-of-plane demagnetizing field, and  $H_{k\perp}$  as the free layer perpendicular interface anisotropy field corresponding to  $2K_{in}/M_s t$ . Therefore, assuming  $H_d$  is  $4\pi M_s$  in all areas,  $H_d - H_{k\perp}$  is 5106 Oe, 4317 Oe and 2765 Oe for 2.00 nm, 1.90 nm and 1.73 nm free layers, respectively. It means that the effective out-of-plane demagnetizing field is highly reduced. This can affect the STT switching in two aspects: the reduction in  $J_{c0}$  and the canted local magnetization on edges.

First of all, it has been shown that for in-plane MTJ devices with perpendicular anisotropy, the critical current is given by [15, 16]

$$J_{c0} \approx (2e\alpha M_s t / \hbar\eta)(H_k + (H_d - H_{k\perp})/2), \quad (2)$$

where  $\alpha$  is the free layer damping factor. Equation (2) implies that the thinner the free layer of a device, the more  $H_{k\perp}$  cancels out the demagnetizing field  $H_d$ , thus resulting in a lower critical current density  $J_{c0}$ . We notice this trend in figure 2 as the curves for the devices with thinner free layers are shifted further left towards lower current densities. This lowering of  $J_{c0}$  allowed us to apply higher  $J/J_{c0}$  ratio before reaching the barrier breakdown limit.

Second, in the localized areas of devices such as the two edges of free layer along the long axis, the demagnetizing effect that keeps the magnetization in-plane is weaker. Therefore, when there is a large interface perpendicular anisotropy component present, the local magnetization on the two ends of the long axis may start to cant out of plane very easily. It is possible that these areas could act as the magnetization nucleation points of STT switching because of the larger initial angle  $\theta_0$  between the free layer and the pinned layer. Ultrafast switching of the entire free layer may be driven by the quick onset of switching at these hotspots.

In conclusion, we demonstrated ultrafast STT switching of 165 ps and 190 ps with 50% and 98% switching probabilities, respectively, in conventional MgO MTJ structures without field assistance. No plateau of switching probability versus pulse width appeared in our data as found in some metallic SVs for sub-ns STT switching. Our device also showed a 101% TMR ratio and room temperature thermal stability factor of more than  $65k_B T$ , which make it a good candidate for STT-RAM application. The effect of free layer thickness on ultrafast switching performance was discussed and we found 190–195 ps switching in both AP-P and P-AP testing from the same sample.

## Acknowledgments

This work was supported by the DARPA STT-RAM program (Grant No HR0011-09-C-0114), the NSF MRSEC Program at

Minnesota (Grants No DMR-0819885) for AL and YSZ and the Intel STT-RAM program for HZ and JPW at University of Minnesota. JPW would also like to thank the useful discussion with Dr B Doyle and Dr Charles Kuo from Intel.

## References

- [1] Devolder T, Chappert C, Katine J A, Carey M J and Ito K 2007 *Phys. Rev. B* **75** 064402
- [2] Bedau D, Liu H, Bouzaglou J J, Kent A D, Sun J Z, Katine J A, Fullerton E E and Mangin S 2010 *Appl. Phys. Lett.* **96** 022514
- [3] Devolder T, Crozat P, Kim J V, Chappert C, Ito K, Katine J A and Carey M J 2006 *Appl. Phys. Lett.* **88** 152502
- [4] Beaujour J M L, Bedau D B, Liu H, Rogosky M R and Kent A D 2009 *Proc. SPIE* **7398** 73980D
- [5] Lee O J, Pribiag V S, Braganca P M, Gowtham P G, Ralph D C and Buhrman R A 2009 *Appl. Phys. Lett.* **95** 012506
- [6] Papusoi C, Delaet B, Rodmacq B, Houssameddine D, Michel J P, Ebels U, Sousa R C, Buda-Prejbeanu L and Dieny B 2009 *Appl. Phys. Lett.* **95** 072506
- [7] Aoki T, Ando Y, Oogane M and Naganuma H 2010 *Appl. Phys. Lett.* **96** 142502
- [8] Zhao H *et al* 2011 *J. Appl. Phys.* **109** 07C720
- [9] Liu H, Bedau D, Backes D, Katine J A, Langer J and Kent A D 2010 *Appl. Phys. Lett.* **97** 242510
- [10] Rowlands G *et al* 2011 *Appl. Phys. Lett.* **98** 102509
- [11] Ikeda S, Miura K, Yamamoto H, Mizunuma K, Gan H D, Endo M, Kanai S, Hayakawa J, Matsukura F and Ohno H 2010 *Nature Mater.* **9** 721–4
- [12] Amiri P K, Zeng Z, Langer J, Zhao H, Rowlands G, Chen Y J, Krivorotov I, Wang J P, Jiang H and Katine J 2011 *Appl. Phys. Lett.* **98** 112507
- [13] Upadhyaya P, Amiri P K, Kovalev A, Tserkovnyak Y, Rowlands G, Zeng Z, Krivorotov I N, Jiang H and Wang K L 2011 *J. Appl. Phys.* **109** 07C708
- [14] Tai M *et al* 2010 *IEEE Trans. Magn.* **46** 2322–7
- [15] Sun J Z 2000 *Phys. Rev. B* **62** 570
- [16] Liu L, Moriyama T, Ralph D C and Buhrman R A 2009 *Appl. Phys. Lett.* **94** 122508